JOURNAL OF MATERIALS SCIENCE 22 (1987) 973–980

Mechanical behaviour of MgO-partially stabilized ZrO_2 ceramics at elevated temperatures

P. F. BECHER
Metals and Ceramics Division, Oak Ridge National Laboratory, Oak Ridge, Tennessee 37831, USA

M. K. FERBER
Ceramic Engineering Department, University of Illinois, Urbana, Illinois 61801, USA

Transformation toughened partially stabilized zirconia ceramics containing magnesia exhibit quite high fracture toughness ($K_{IC} \geqslant 8\,MPa\,m^{1/2}$) at temperatures of up to 500° C. The observed temperature dependences of the toughness and the fracture strength are consistent with that of the transformation behaviour. The high toughness of these materials results in a significant reduction in the sensitivity of the flexure strength to crack size increases. Exposure of these materials at 1000° C for prolonged periods results in flexure strength changes associated with the generation of the monoclinic phase by tetragonal precipitate destabilization and eutectoid decomposition. However, when exposed at 500° C, neither the phase contents nor the flexure strength are altered for exposures of up to 1000 h.

1. Introduction

Ceramics which exhibit high fracture toughness and strength levels from the stress induced phase transformation of the tetragonal zirconia (or hafnia) phase are of considerable interest for a variety of structural applications involving tensile stresses. Such toughened ceramics include partially stabilized zirconias, fine-grained tetragonal zirconias, and other ceramics containing tetragonal zirconia as a second phase. Commercial transformation toughened zirconia ceramics typically use stabilizers of MgO, CaO, or Y_2O_3. The MgO or CaO partially stabilized zirconia (PSZ) consist of 40 to 60 μm cubic (c) grains containing a second phase of finely dispersed, submicrometre tetragonal (t) and monoclinic (m) ZrO_2 phase precipitates. On the other hand, the Y-doped zirconia microstructures typically contain $< 5\,\mu$m grains which are predominately the tetragonal (t) ZrO_2 phase.

The tetragonal phase which is present in both types of zirconia is generally metastable at temperatures well below 1000° C, which is the approximate temperature at which pure zirconia transforms to the monoclinic phase. This transformation of the tetragonal to the monoclinic phase is accompanied by a volume increase and a shear strain. Consequently, at room temperature, applied tensile stresses such as those in the vicinity of a crack tip are required to initiate the transformation of the t to the m phase. The transformation in the zone surrounding the crack lowers the stress intensity at the crack tip such that a higher applied stress intensity K_{Ia} is required for fracture than the K_{Ia} required in the absence of such a transformation zone. Several studies [1, 2] have shown that if one considers only the volume expansion or dilational component of the transformation strain ($e^T \simeq 0.03$) that the resulting critical fracture toughness, K_{IC}, is

$$K_{IC} = K_{IC}^M + AV_f E^c e^T (r_T)^{1/2} \quad (1)$$

where K_{IC}^M is the toughness of the matrix in the absence of the transformation, A is a constant related to the stress state triggering the transformation, V_f is the volume fraction of t-phase participating in the transformation, E^c is the modulus of elasticity (E^c for PSZ is ~ 200 GPa), and r_T is the zone width. The zone size is also related to the critical transformation stress, σ_c^T by

$$\sigma_c^T = K_{IC}/(Br_T)^{1/2} \quad (2)$$

where B is a constant.

The critical stress associated with the (t) to (m) transformation is primarily dictated by the nucleation characteristics which are not fully understood. Nevertheless, a resonable estimate of σ_c^T can be obtained from the external strain energy change ΔU_{SE} accompanying the stress driven transformation which has the form,

$$\Delta U_{SE} = (\Delta S^{t-m})(T - M_s) = \sigma_c^T e^T \quad (3)$$

where T is the test temperature, ΔS^{t-m} is the change in entropy and M_s is the temperature at which the transformation begins (upon cooling) in the absence of an applied stress [3–5]. Since any transformation toughening requires that the overall $\Delta U_{SE} > 0$ at $T > M_s$ for the stress driven transformation, rearrangement of Equation 3 yields

$$\sigma_c^T = \Delta S^{t-m}(T - M_s)/e^T \quad (4)$$

0022–2461/87 $03.00 + .12

and σ_c^T will equal zero when $T = M_s$ and increase with increasing test temperature or decreasing M_s value. As shown previously this relationship is descriptive of the behaviour of at least the PSZ ceramics [4].

Although with proper processing, PSZ ceramics can exhibit high critical strength and toughness at temperatures of 500° C and below, several questions arise as to their behaviour at low stresses and after, for prolonged periods of exposure of elevated temperatures. For example, limited studies [6] suggest that for certain stress regimes PSZ ceramics may be subject to slow crack growth and thus, strength degradation. In addition, at temperatures above 500° C, time-dependent ageing effects [7–10] can reduce the concentration of the (t) phase involved in the stress-induced transformation leading to significant losses in both strength and toughness. Because the long-term mechanical reliability at elevated temperature can be a key requirement for application of ceramic materials such as in engine components, it is essential that any changes in mechanical properties be well understood. This paper reports the results of recent studies aimed at examining the critical fracture strength and toughness, and the fatigue-ageing properties of two types of commercial MgO–PSZ ceramics.

2. Experimental procedure

Two commercial Mg–PSZ ceramics (Nilcra Ceramics, St Charles, Illinois, USA) designated TS-PSZ (a moderately high toughness thermal shock grade) and a MS–PSZ (a high toughness, high fracture strength grade) were chosen for testing. These materials were obtained in the form of circular discs 100 mm diameter and 7.6 mm thick. Rectangular bend specimens (25.4 mm × 2.82 mm × 2.5 mm) were then machined from the discs for subsequent mechanical property studies. The tensile surface of each sample was polished to a 0.25 μm finish to minimize any surface compressive stresses which can be introduced by the t → m transformation brought about by the stresses generated by more severe finish operations. The edges were bevelled using a 6 μm diamond wheel to eliminate edge defect/cracks.

Critical fracture strengths were obtained in four-point flexure (6.35 mm × 19.05 mm inner to outer spans) at a stressing rate of 345 MPa sec^{-1} in air over the temperature range 22 to 1000° C. Critical fracture toughness values were derived from the fracture strength and final crack sizes of flexure specimen containing at least 0.93 N Vicker's indents in the maximum stress region of the tensile surface [11]. Note that this method requires that fracture initiates from one of the indent cracks normal to the tensile axis. The validity of these results was verified by K_{IC} values obtained at 22° C with the applied moment double cantilever beam technique.

The fatigue-ageing behaviour was determined using an interrupted fatigue (IF) technique in which the four-point bend strength, σ_f, was measured as a function of time, t, temperature, T, and applied stress, σ_{IA}. This method has several advantages over conventional static fatigue testing. First, since time is a controllable quantity, problems associated with an unpredictable fatigue life (as in the case of static fatigue) are avoided. In the present study, this feature allowed for periodic examination of test specimens so that changes in both phase composition and transformation characteristics could be ascertained. A second advantage is that processes responsible for both strength degradation and strength enhancement can be readily distinguished [12].

Interrupted fatigue studies involving both materials were conducted at temperatures of 500 and 1000° C for exposure times ranging from 1 to 1000 h. Some data were established using specimens that were not subjected to an applied stress (i.e. $\sigma_{Ia} = 0$); however, most tests were performed with σ_{Ia} equal to approximately 55% of the fast fracture strength, σ_f, value measured at the same T for a hold time of 0.5 h. For each test condition, σ_f was determined at temperature by fracturing several samples.

All testing was conducted in a specially designed flexure test system (FTS) (based on a similar system originally developed by N. J. Tighe of the National Bureau of Standards) capable of holding up to three bend samples. The general layout of the FTS is shown in Fig. 1. The test frame contains the hardware for applying mechanical forces to each of three samples which are supported by Al_2O_3 four-point bend fixtures. The loads are generated by pneumatically driven air cylinders located at the top of the support frame. These loads are transmitted into the hot zone of the furnace through (Al_2O_3) rods. Each of the bottom three Al_2O_3 rods is also attached to a load cell which monitors the applied force as a function of time. Water-cooled adapters connect the aluminium oxide rams to both the load cells and the air cylinders. The computer monitors the load on each specimen and provides necessary adjustments in the air pressure (via the electropneumatic transducer) such that the desired stress level is maintained. Following the designated exposure time, the samples are fractured using a prescribed loading rate (345 MPa sec^{-1} in the present study).

Several techniques were used to characterize the as-received materials and tested IF samples. For example, the microstructures were examined using both standard ceramographic methods and scanning electron microscopy (SEM). The volume fractions of the cubic (c), tetragonal (t), and monoclinic (m) phases were determined from X-ray diffraction and laser Raman spectroscopy studies.

The thermal expansion of the MS and TS ceramics was determined using a dual rod dilatometer (Dilatronic II, Theta Industries, Inc., Port Washington, New York). The reference standard consisted of an NBS single crystal Al_2O_3. In order to establish the M_s temperature in the as-received materials, the dilatometer was modified so that temperatures as low as −190° C could be achieved [4]. Finally, the expansion–contraction characteristics were also measured for selected IF samples. The resulting data (per cent elongation plotted against temperature) were used to examine changes in the (t) → (m) transformation characteristics arising from the high-temperature exposure.

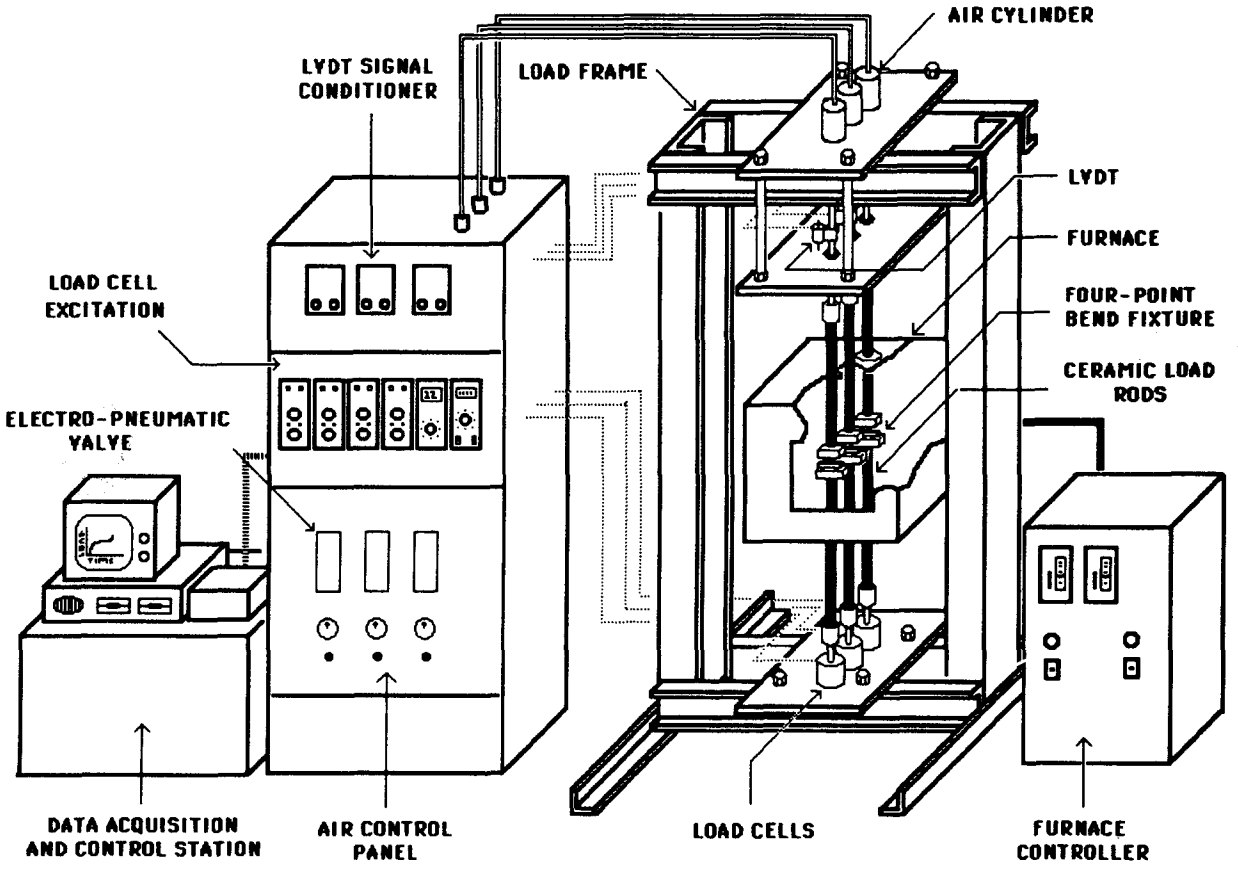

Figure 1 General schematic of flexure test system.

3. Results and discussion

3.1. Critical fracture toughness and strength

The microstructures of the TS and MS–PSZ ceramics generally consisted of approximately 50 μm grains containing fine ($< 0.1 \times \leqslant 0.4\,\mu$m) (t) precipitates (Fig. 2). The larger grain-boundary precipitates (possibly monoclinic) were characteristic of both materials. Although not shown in this figure, considerable porosity was also observed in both microstructures. Finally, microprobe studies indicated that the two PSZ ceramics contained MgO and HfO_2 at concentrations of 8.4 and 1.0 mol %, respectively.

X-ray analysis of the polished surfaces of the as-received MS- and TS-PSZ materials revealed monoclinic ZrO_2 contents of 7 and 15%, respectively. The calculations were based on equations given by Porter and Heuer [13]. Unfortunately, the volume fractions for the (c) and (t) phases could not be determined using this technique because of overlapping of the cubic (1 1 1) and tetragonal (1 0 1) peaks. However, additional laser Raman spectrographic studies provided independent estimates of the ratio of tetragonal to the monoclinic plus tetragonal content. These numbers were then used in conjunction with the X-ray data to yield the approximate phase analysis:

TS-PSZ: 25 to 28% tetragonal, 15% monoclinic, $\leqslant$55% cubic

MS-PSZ: 35 to 39% tetragonal, 7% monoclinic, $\leqslant$56% cubic

The temperature dependence of the critical fracture toughness of the TS- and MS-PSZ ceramics is

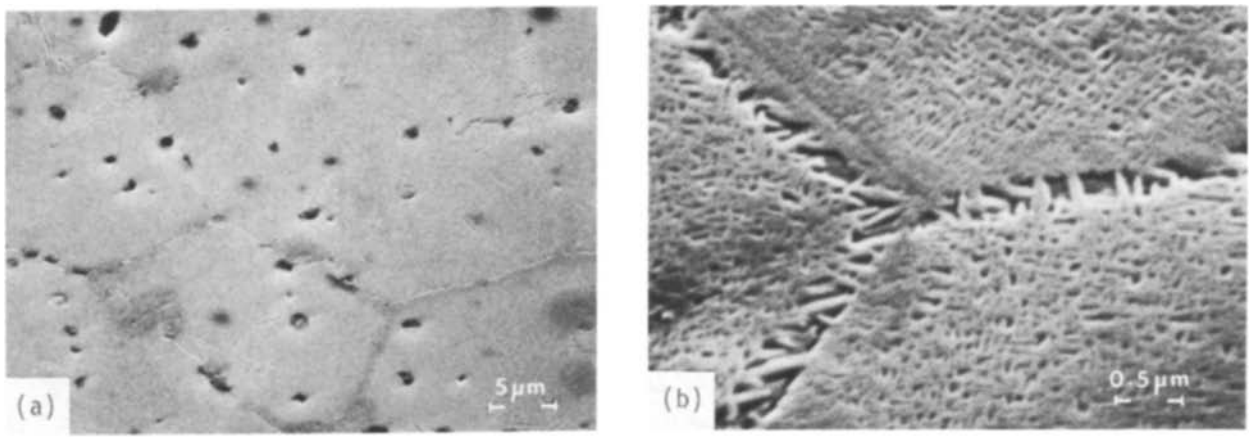

Figure 2 Typical microstructure of both PSZ ceramics consists of large ($\sim 50\,\mu$m) grained cubic matrix (a) with fine intergranular and coarser intragranular precipitates (b). Etched microstructure obtained with 20% HF solution.

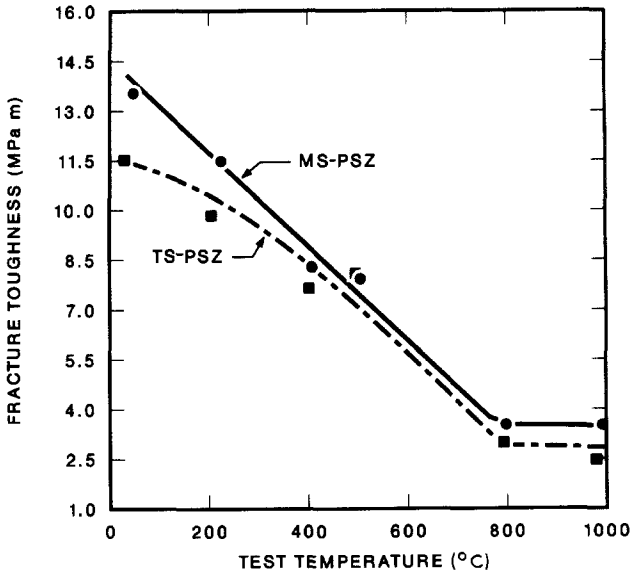

Figure 3 The critical fracture toughness of each PSZ ceramic decreases with increasing temperature. Toughness values of $\geqslant 8\,\text{MPa}\,\text{m}^{1/2}$ are maintained within a temperature range of 22 to 500° C.

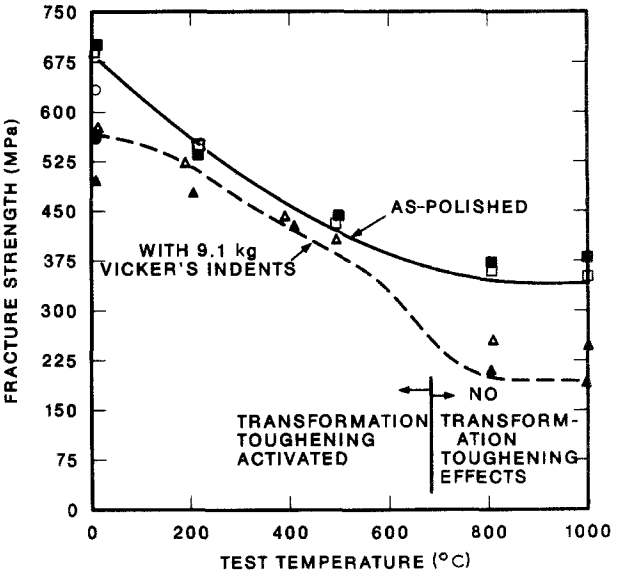

Figure 4 The fracture strength of partially stabilized ZrO_2 ceramics is quite insensitive to surface damage. At $\leqslant 500°$ C, the four-point flexure strengths of MS and TS grades of PSZ ($K_{IC} \geqslant 12\,\text{MPa}\,\text{m}^{1/2}$ at 22° C) are not substantially lowered when high load (4.6 and 9.1 kg) Vicker's indents are introduced in the tensile surfaces. In this temperature range, the PSZ ceramics exhibit transformation toughening ($K_{IC} \geqslant 8\,\text{MPa}\,\text{m}^{1/2}$ at $\leqslant 500°$ C). At $\geqslant 800°$ C the strengths are lowered approximately two-fold consistent with the absence of transformation toughening ($K_{IC} \sim 3\,\text{MPa}\,\text{m}^{1/2}$). Indent load (kg): (■, □) 0; (○, ●) 4.6; (△, ▲) 9.1. (■, ○, △) MS grade; (□, ●, ▲) TS grade.

illustrated in Fig. 3. Both materials exhibit a decrease in toughness with increasing test temperature and the MS-PSZ exhibits higher K_{IC} values in the lower temperature region. However, below 500° C, both of these materials exhibit K_{IC} values of $8\,\text{MPa}\,\text{m}^{1/2}$ or greater.

If we examine the relationships of toughness to the parameters discussed in Section 1 and refer to Equations 1 to 3, we can derive the following relation:

$$K_{IC} = K_{IC}^{M}[1 + AB^{1/2}V_f E^c(e^T)^2/\Delta S(T - M_s)] \quad (5)$$

for the critical fracture toughness of the PSZ ceramics. This indicates that K_{IC} will increase as V_f increases and M_s approaches T where $T > M_s$. Note that the other parameters are equivalent for the two PSZ ceramics studied here. At a T of 22° C, the MS-PSZ should have a somewhat higher K_{IC} value than the TS-PSZ based solely on the higher V_f level of the tetragonal content in the MS-PSZ. However, this assumes that the M_s temperatures of the two materials are equivalent. The thermal expansion data indeed showed that the M_s is $-50 \pm 5°$ C for the stable tetragonal phase (i.e. that present in both of these materials at 22° C). Therefore, the differences in toughness values at low temperatures are due to differences in V_f and not differences in the M_s temperatures which reflect differences in the ease of transforming the tetragonal phase [4].

The decrease in K_{IC} with increase in test temperature, however, is a result of the increase in the $(T - M_s)$ term in Equation 5. In other words, it becomes increasingly more difficult to transform the tetragonal phase as T is increased (i.e. the tetragonal phase is the more thermodynamically stable phase at elevated temperatures). At $T \geqslant 800°$ C, no, or very little, stress-induced transformation toughening occurs.

Looking at the critical fracture strengths of these materials (Fig. 4), we see that the strength decreases with increasing temperature in a manner comparable to that of the toughness. Thus the toughness is the dominant term in the observed strength.

The high toughness of these PSZ materials is perhaps best reflected by the very small degradation in fracture strength when large initial indents and ($> 400\,\mu$m) flaws were purposely introduced with the 0.93 N Vicker's indents at loads up to 0.93 N. As seen in Fig. 4, the fracture strength of these indented PSZ samples is only slightly degraded as compared to that for the as-polished samples containing only natural flaws (e.g. pores, cracks) over the temperature range in which substantial transformation toughening occurs. Conventional ceramics such as commercial sintered alumina ceramics which have a fracture toughness of approximately $3.5\,\text{MPa}\,\text{m}^{1/2}$ exhibit at least a 2 to 2.5-fold decrease in fracture strength (σ_f for unindented samples is $\sim 630\,\text{MPa}$) when similar indent loads are used to introduce cracks. Furthermore, sapphire (single crystal α-Al_2O_3) which has a lower K_{IC} ($\sim 1.8\,\text{MPa}\,\text{m}^{1/2}$) exhibits a three-fold loss in strength (σ_f is 650 MPa as polished and annealed) with only a 0.02 N Vicker's indent.

The flaw diameters, d, for the fracture of the as-polished samples without indent cracks, estimated for semi-circular surface cracks ($K_{IC} = Y\sigma_f C_f^{1/2}$ where Y is approximately 1.6 and $C_f = d/2$), are approximately 440, 335 and 240 μm for tests at 22, 500 and 800° C, respectively. On the other hand, the measured final total surface flaw lengths after fracturing the PSZ ceramics samples containing the indent cracks at 22, 500 and 1000° C increase to 600, 500 and 440 μm, respectively. This increased flaw size is responsible for the minor loss in the strength of indented samples for $T < 800°$ C. However, these toughened materials show excellent outstanding ability to withstand strength degradation in these

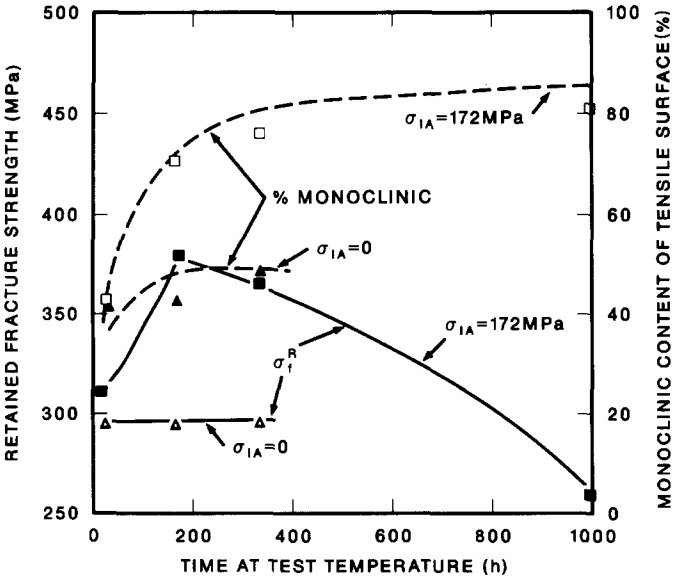

Figure 5 TS–PSZ ceramic exhibits changes in fracture strength at 1000° C and increase in room temperature monoclinic content when subjected to a stress of 173 MPa at 1000° C with increase in time of exposure. The unstressed material does not undergo changes in strength at 1000° C and exhibits only a small increase in monoclinic content with increase in exposure time.

cases where further flaw generation surface damage can occur.

3.2. Ageing effects on the high temperature fracture strength and phase content of PSZ behaviour at 1000° C

3.2.1. Behaviour at 1000° C

The fracture strengths retained at 1000° C for the TS grade PSZ after various exposure times in the IF tests at 1000° C are shown in Fig. 5. Note first that when the applied stress during the exposure is 172 MPa ($\sim 55\%$ σ_f) that there is a maximum in the retained strength with increasing exposure time. This maximum is absent in the unstressed TS-PSZ. However, both the stressed and unstressed MS-PSZ ceramic exhibit a similar maximum in the retained fracture strength at 1000° C with increase in exposure time at 1000° C (Fig. 6).

These observed maxima in the retained fracture strengths are accompanied by a large increase in the room-temperature monoclinic phase contents of the tensile surface after testing (Figs 5 and 6). On the other hand, no or very little increase in such monoclinic contents is detected when the retained fracture strength at 1000° C is unaltered with exposure time, unstressed TS PSZ data in Fig. 5. These increases in monoclinic phase content after testing at 1000° C are not a result of transformation toughening during the test. As shown in Fig. 3, neither PSZ ceramic exhibits transformation toughening at 800° C or above. Simply annealing unstressed samples at 1000° C without fracturing them results in an increase in room temperature monoclinic phase content (to 30% monoclinic phase). Thus ageing effects similar to those observed after ageing at 1100° C [7–9] are suspected to be influencing the strengths and phase contents.

The studies of Hannink and co-workers [7–10] show that ageing at 1100° C yields monoclinic phase grains and MgO by the eutectoid decomposition of cubic ZrO_2. This reaction generally initiates at the cubic phase grain boundaries and propagates into the grain interiors consuming the cubic grain and the precipitates present within them. The thermal expansion anisotropy of the monoclinic grains and the expansion mismatch with the cubic phase eventually promote microcracking at extended ageing times.

The second change observed by these same authors [7–9] was the loss of coherency of the tetragonal precipitate–cubic matrix interface due to MgO segregation and delta-phase ($Mg_2Zr_5O_{12}$) formation. This

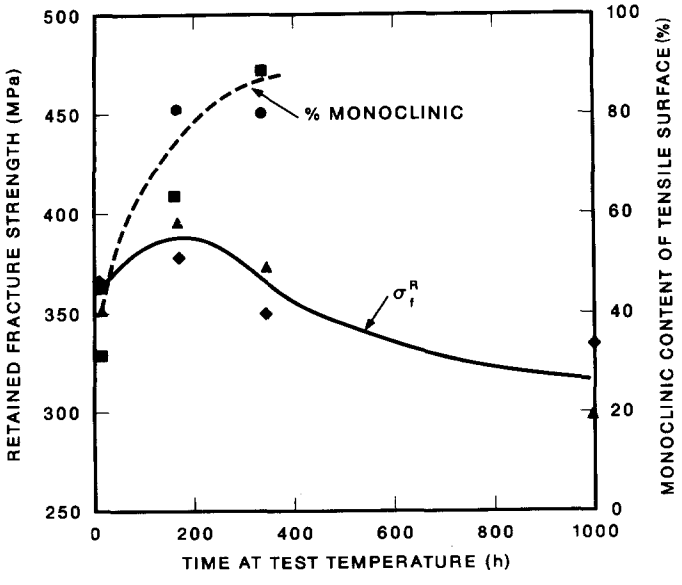

Figure 6 MS–PSZ ceramic exhibits a maximum in fracture strength at 1000° C and an increase in room temperature monoclinic content when held at 1000° C. Similar changes in both retained fracture strength and monoclinic content occur with increase in exposure time when samples are subjected to applied stresses of (▲, ●) 0 and (◆, ■) 172 MPa.

process destabilizes a portion of the tetragonal phase precipitates and yields some precipitates which have a higher martensite start temperature (M_s). This process is indicated in our study by the thermal expansion behaviour of the stressed (and unstressed) TS-PSZ samples after the IF tests at 1000° C. The thermal expansion behaviours of these TS-PSZ samples exhibit an additional hysteresis loop within the temperature range 22 to 700° C due to the conversion of a portion of the originally stable precipitates to the destabilized form resulting in an increase in monoclinic phase content at 22° C. Thus such materials after exposure exhibit three types of tetragonal phase: those with $M_s < 22°$ C, those with 22° C $< M_s <$ 700° C, and those with $M_s >$ 1000° C.

While even the as-received TS material exhibits a small hysteresis in the 22° C $< T <$ 700° C range, the hysteresis strain associated with these unstable precipitates increases with increase in exposure times up to 336 h at 1000° C. Note that the TS-PSZ ceramic is originally aged at about 1100° C to develop such destabilized precipitates and improve its thermal shock resistance as part of the fabrication process. The TS-PSZ ceramics from the IF tests at 1000° C then show an increase in destabilized precipitates with increasing exposure time. Yet these precipitates will exist in the tetragonal phase at 1000° C as they are fully converted to the tetragonal phase at 650 to 750° C.

However, additional thermal expansion data for the IF test samples of the stressed TS-PSZ show a hysteresis loop representing a monoclinic phase which is still present at $\geqslant$ 1000° C. This phase has an M_s temperature of approximately 800° C. This represents the transformation of monoclinic phase which exists at the 1000° C test temperature. We can now use the thermal expansion data and the room temperature ZrO_2 phase contents obtained from X-ray diffraction in conjunction with calculated linear transformation strains to determine the relative amounts of the stable and destabilized precipitates and the high temperature monoclinic phase.

The thermal expansion data provide the hysteresis strain associated with each hysteresis loop due to each transformation occurring over different temperature ranges. This can then be compared to the linear hysteresis strain (e_h) expected for the content of monoclinic and stable tetragonal phase detected at 22° C based on e_h which is the product of the volume fraction of the particular phase and $e^T/3$. The comparable strain associated with the destabilized precipitates, $M_s \sim$ 300° C and $A_f \sim$ 700° C, is obtained from the thermal expansion data in the 22 to 1000° C range. The strain associated with the stable tetragonal precipitates, $M_s <$ 22° C, can be obtained by low temperature expansion data and by using the volume fraction of the tetragonal phase at 22° C and e^T. The difference between the linear hysteresis strain obtained from the product of the total monoclinic content at 22° C times $e^T/3$ and the measured linear hysteresis strain for the transformation occurring between 22 and 700° C determines the hysteresis strain for and thus volume fraction of, the monoclinic phase which exists at 1000° C. These results are shown in Table I for the as-received MS and TS-PSZ ceramics and the stressed and unstressed TS-PSZ after the 1000° C IF tests.

These data indicate that both the eutectoid

TABLE I Linear transformation strains for various PSZ samples

Linear transformation strain	MS grade PSZ As-received	TS grade PSZ					
		As-received	After IF test at 1000° C				
			$\sigma_1 = 55\%\ \sigma_f$			$\sigma_{Ia} = 0\%\ \sigma_f$	
			$t = 24$ h	$t = 168$ h	$t = 1000$ h	$t = 24$ h	$t = 336$ h
(A) *Thermal expansion results*							
e_h (%) for							
(1) $M_s < 22°$ C	> 0.1*	> 0.1*	0.09*	0	0		
(2) $M_s > 22°$ C but $< 500°$ C	0.07	0.16	0.29	0.50	0.27	0.45	0.45
(B) *Calculated* $e_h = V_f(e^T/3)$ $e^T = 3\%$							
(3) for $M_s < 22°$ C							
V_f = t-phase fraction	0.37	0.27	$\leqslant$ 0.05	0	0	< 0.05	0
e_h (%)	0.37	0.27	$\leqslant$ 0.05	0	0	< 0.05	0
(4) for $M_s > 22°$ C							
V_f = m-phase fraction	0.07	0.15	0.39	0.70	0.85	0.40	0.45
e_h (%)	0.07	0.15	0.39	0.70	0.85	0.40	0.45
(5) V_f of m-phase at 1000° C from $\frac{e_{h_4} - e_{h_2}}{e^T/3}$ †	–	–	0.10	0.20	0.58	–	–

*For tetragonal precipitates with $M_s < 22°$ C, lower temperature limitation of dilatometer (−190° C) is not sufficient to reach M_f temperature where all precipitates are converted to monoclinic (m) phase. Thus E_h is underestimated.

† e_{h_4} and e_{h_2} obtained from steps (A2) and (B4).

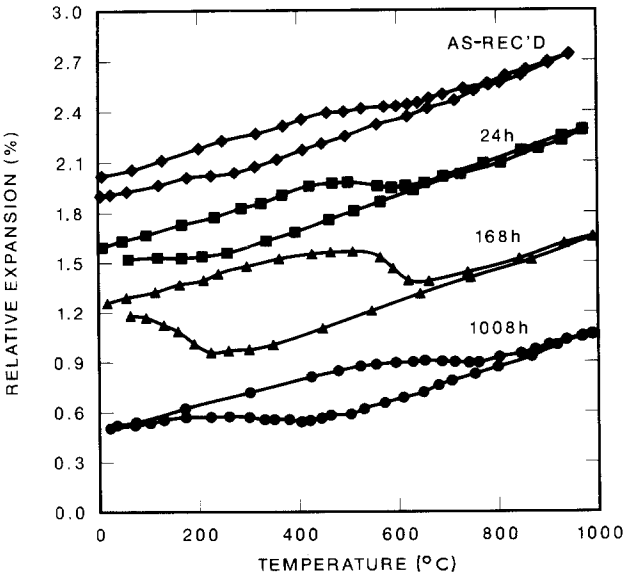

Figure 7 Thermal expansion curves of TS–PSZ illustrate changes in hysteresis due to tetragonal $\rightleftharpoons$ monoclinic transformation for samples held at 1000° C at an applied stress of 172 MPa for various exposure times. The increase in the hysteresis at temperatures between 22 and approximately 700° C is due to the destabilization of the tetragonal precipitates with increasing duration of 1000° C exposure. After the 1008 h exposure there is a decrease in the hysteresis associated with this intermediate temperature transformation.

decomposition reaction and delta-phase formation coupled with destabilization of the precipitates are activated during the 1000° C IF tests of the TS-PSZ. As seen in Fig. 5, these processes result in very high room temperature monoclinic contents at exposure times $\geqslant 24$ h in the stressed TS material. The results in Table I show that this increase in monoclinic phase content with exposure time is associated with a continuous increase in the high temperature monoclinic phase brought about by the eutectoid reaction with exposure time. In addition, there is an initial increase in the destabilized precipitate content which then decreases for exposure times > 336 h, most likely due to its consumption by the continued eutectoid reaction as observed by others [7–9]. The similarities in the large increase in monoclinic content in the MS-PSZ after the IF test at 1000° C (Fig. 6), are indicative of comparable phase reactions and changes in this material.

However, the unstressed TS-PSZ IF tests at 1000° C result in only a modest increase in the destabilized precipitate content and not the large increase in monoclinic phase associated with the eutectoid decomposition detected in the previous results. The reasons for this lack in the formation of the high temperature monoclinic in the unstressed TS-PSZ are not clear. However, it is clear that when this occurs that the 1000° C retained strengths remain constant with increasing exposure time. Thus the increase in destabilized precipitates observed in the unstressed TS-PSZ test has little, if any, influence on the strength retained at 1000° C. On the other hand, the generation of destabilized precipitates does alter the mechanical properties obtained at room temperature [7–9].

These results and those for the MS and the stressed TS-PSZ ceramics reveal that the initial increase in retained strengths noted in Figs 5 and 6 must be due to the appearance of the high temperature monoclinic phase (and MgO) as a second phase. With further increase in this monoclinic phase content, exposure time > 168 h, the retained strengths are representative of a monoclinic phase matrix at 1000° C and not a cubic phase matrix. The retained strengths then decrease in the high monoclinic phase matrix materials at these longer exposure times in these TS and MS samples. The microcracking in these latter materials observed here and by others [7–9] can also contribute to further loss in retained strengths with the longer exposure times.

3.2.2 Behaviour at 500° C

The results of the IF tests at 500° C for the TS-PSZ stressed at 55% of the critical fracture stress at this same temperature are depicted in Fig. 8. The retained fracture strengths and the tensile surface room temperature monoclinic phase content after testing remain constant with increasing time of exposure. The PSZ ceramics are apparently quite stable at 500° C, unlike their behaviour at 1000° C.

However, one sees that the monoclinic phase contents after the 500° C IF tests are considerably higher than in the as-received TS material, ~33% and 15%, respectively. This higher monoclinic content after testing is a result of the stress-induced transformation which occurs during fracture at 500° C. This is noted in the high critical fracture toughness (8 MPa $m^{1/2}$) of this material in the as-received condition at 500° C (Fig. 3). The fact that the 500° C exposures with a relatively high applied stress after 1000 h do not alter the amount of the monoclinic phase resulting from the stress-induced transformation during fracture, further attests to the stability of the properties and phases of these materials at 500° C.

4. Conclusions

The two high tetragonal phase content PSZ ceramics considered here represent materials with exceptionally high fracture toughness, fracture strengths and surface damage resistance over the temperature range of 22° C to at least 500° C. The critical fracture toughness decreases with increasing test temperature but is $\geqslant 8$ MPa $m^{1/2}$ temperatures of $\leqslant 500$° C. The temperature dependence of the toughness is consistent with the thermodynamics of the stress-induced tetragonal to monoclinic phase transformation. Thus the toughness increases as the term $(T - M_s)$ decreases where T is the test temperature and M_s is the temperature at which the tetragonal to monoclinic transformation initiates on cooling.

The phase contents are altered by increase in the time the samples were subjected to 1000° C with and without an applied stress. With short exposure times ($\leqslant 168$ h), both the TS and MS grades of the PSZ exhibit an increase in monoclinic phase due to the formation of unstable precipitates (M_s is increased to ~300° C from −50° C) as a result of MgO segregation and delta phase $Mg_2Zr_5O_{12}$ generation. In the MS- and stressed TS-PSZ ceramics, this is accompanied by ever increasing generation of monoclinic phase which is stable at 1000° C. The samples which

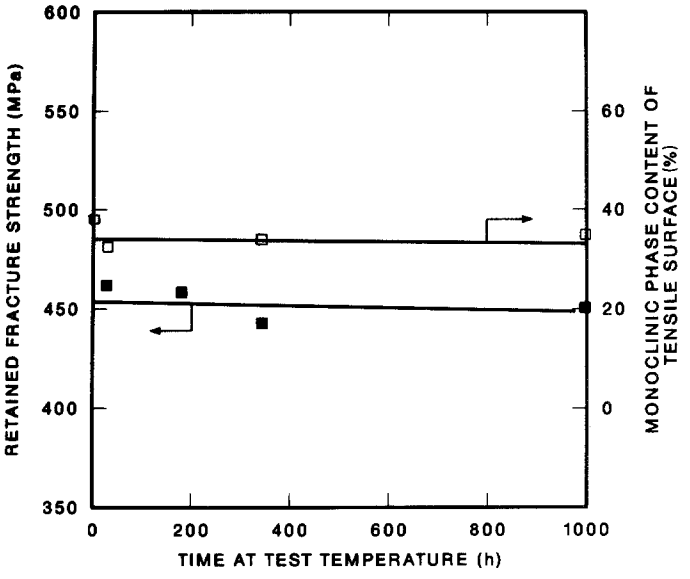

Figure 8 Even when subjected to an applied stress of 248 MPa at 500° C, the TS–PSZ does not exhibit changes in strengths retained at 500° C or in room temperature monoclinic content.

exhibit the latter phase formation are subject to changes in the fracture strengths retained at 1000° C after the 1000° C exposures for times of up to 1008 h. The TS-PSZ aged at 1000° C with no applied stress exhibits only the generation of unstable precipitates and thus shows no change in retained fracture strength with increase in exposure time. The mechanical properties of these materials can thus be altered with long-term exposures at 1000° C.

However, the fracture strengths at 500° C and the phase contents are not altered by exposure to an applied stress at 500° C for times of up to 1000 h. At this temperature the materials exhibit considerable transformation toughening. Thus the materials have excellent potential for structural applications to temperatures of at least 500° C.

Acknowledgement

This Research was sponsored by the Advanced Materials Development Program, Office of Transportation Systems, US Department of Energy, under contract DE-AC05-840R21400 with Martin Marietta Energy Systems, Inc.

References

1. D. MARSHALL, A. G. EVANS and M. DRORY, Transformation Toughening in Ceramics, in "Fracture Mechanics of Ceramics", Vol. 6, edited by R. C. Bradt, A. G. Evans, D. P. H. Hasselman and F. F. Lange (Plenum, New York, 1983) pp. 289–307.
2. A. G. EVANS, Toughening Mechanisms in Zirconia Alloys, in "Fracture in Ceramics Materials", edited by A. G. Evans (Noyes, New Jersey, 1984) pp. 15–55.
3. C. A. ANDERSON and T. K. GUPTA, Phase Stability and Transformation Toughening in Zirconia, in "Science and Technology of Zirconia, Advances in Ceramics", Vol. 3, edited by A. H. Heuer and L. W. Hobbs (American Ceramic Society, Ohio, 1981) pp. 184–201.
4. P. F. BECHER, M. V. SWAIN and M. K. FERBER, *J. Mater. Sci.* **22** (1987) 76.
5. N. CLAUSSEN and M. RUHLE, Design of Transformation Toughened Ceramics, in "Science and Technology of Zirconia, Advances in Ceramics", Vol. 3, edited by A. H. Heuer and L. W. Hobbs (American Ceramics Society, Ohio, 1981) pp. 137–63.
6. V. J. TENNERY, M. K. FERBER, P. F. BECHER and S. B. WATERS, in "Proceedings of the Twenty-Second Automotive Technology Development Contractors' Coordination Meeting P-155" (Society of Automotive Engineers, Warrendale, Pennsylvania, March 1985) pp. 409–18.
7. R. HANNINK and M. SWAIN, *J. Aust. Ceram. Soc.* **18** (1983) 53.
8. R. HANNINK and R. GARVIE, *J. Mater. Sci.* **17** (1982) 1637.
9. R. HANNINK, *ibid.* **18** (1982) 457.
10. M. V. SWAIN, R. C. GARVIE and R. H. J. HANNINK, *J. Amer. Ceram. Soc.* **66** (1983) 358.
11. R. COOK and B. R. LAWN, *Amer. Ceram. Soc. Commun.* **11** (1983) 200.
12. S. M. WIEDERHORN, A Probabilistic Framework for Structural Ceramics, in "Fracture Mechanics of Ceramics", Vol. 5, edited by R. C. Bradt, A. G. Evans, D. P. H. Hasselman and F. F. Lange (Plenum, New York, 1983) pp. 197–226.
13. D. L. PORTER and A. H. HEUER, *J. Amer. Ceram. Soc.* **62** (1979) 298.
14. N. BHATHENA, R. G. HOAGLAND and G. MEYRICK, *ibid.* **67** (1984) 799.

Received 20 January
and accepted 21 July 1986